Building and Environment 45 (2010) 2002–2007

Contents lists available at ScienceDirect

Building and Environment

journal homepage: www.elsevier.com/locate/buildenv

Evaluation of an air-cleaning unit having photocatalytic sheets to remove acetaldehyde from indoor air

M. Sung [a,*], S. Kato [b], F. Kawanami [c], M. Sudo [d]

[a] Department of Architecture, The University of Tokyo, 4-6-1 Komaba, Meguro-ku, Tokyo 153-8505, Japan
[b] Institute of Industrial Science, The University of Tokyo, 4-6-1 Komaba, Meguro-ku, Tokyo 153-8505, Japan
[c] ANDES ELECTRIC Co. Ltd., 1-3-1 Kiyono Kogyodanchi, Hachinohe, Aomori 039-2292, Japan
[d] SOGO SETSUBI Consultant Co. Ltd., 1-34-14 Hatagaya, Shibuya-ku, Tokyo 151-0072, Japan

ARTICLE INFO

Article history:
Received 30 October 2009
Received in revised form
12 March 2010
Accepted 21 March 2010

Keywords:
Photocatalytic oxidation
Air-cleaning
Acetaldehyde
CFD
Radiation

ABSTRACT

A photocatalytic oxidation (PCO) reactor to which newly developed photocatalytic sheets were applied to decontaminate indoor air was considered in this study. Firstly, the PCO reactor was designed to achieve efficient ultraviolet (UV) irradiation. Then the rate at which acetaldehyde, as a representative indoor air contaminant, was removed by the PCO reactor was calculated using a computational fluid dynamics (CFD) simulation. In this process, some alternatives that achieved higher removal performance using obstacles at the inlet and outlet openings were introduced. The results of the CFD simulation showed that the obstacles installed in the middle of the inlet and outlet openings helped to improve the removal performance of the PCO reactor as the degree of contact by the acetaldehyde on the PCO sheets was increased. Furthermore, the results of these experiments also showed some improvement in removal performance when obstacles were installed. However, the overall experimental performances were far lower than as had been suggested by the CFD simulation, which inferred that the oxidation rate on the surface of the PCO sheets was not 100%, as had been assumed in the CFD simulation. Nevertheless, CFD simulations are assumed to be a good method for selecting the optimal option from many alternative PCO reactors.

1. Introduction

Indoor pollutants in buildings are primarily volatile organic compounds (VOCs) and particles of various sizes. Particles are usually removed with filters installed in the air-conditioning units or ventilation systems, while VOCs have also been reduced mainly by source control related to building materials. However there are many potential sources of VOCs in life, and they can be emitted at any time if an appliance that contains VOCs is used in a building. In particular, although overall formaldehyde concentrations have been decreasing since it was declared as a primary indoor air pollutant, concentrations of acetaldehyde, which has been used as an alternative of formaldehyde, have been increasing [1]. Acetaldehyde, which is classified to be a probable carcinogen in humans [2], is considered to cause not only health problems, but also an unpleasant odor [3].

Photocatalytic oxidation (PCO) is considered a promising technology, and has been investigated by many researchers in various fields. In past research, its ability to break down volatile organic compounds in the air has been proven in many instances [4–7]. PCO reactors usually use pure titanium dioxide (TiO_2) or TiO_2 with some metal ions to improve the PCO reactivity, and VOCs are removed through the repeated process of absorption and oxidation reactions of TiO_2 [8]. The photocatalytic oxidation of acetaldehyde is known to produce carbon dioxide during the process as shown in Fig. 1 [9]. In order to activate this process, an ultraviolet A-band (UVA) lamp emitting UV of peak irradiance near 365 nm is generally used. Some researchers indicated that ultraviolet C-band (UVC) lamps emitting at frequencies mostly around 254 nm can also induce effective or more effective reactions of TiO_2 [10,11].

Most previous studies have dealt with the PCO reaction performances using experimental methods, and they were expressed with adsorption models such as the Langmuir–Hinshelwood equation [12,13]. The equation relates the concentration of reaction target compounds to the reaction rate with adsorption isotherm kinetics, and several constants in the equation need to be obtained from a regression process using the experimental data. However, as these constants vary depending on the shape of the PCO reactor, many experiments are also needed. Some numerical approaches have been tried to model radiation fields of PCO monolith reactors

* Corresponding author. Tel.: +81 3 5452 6431; fax: +81 3 5452 6432.
E-mail address: mkii@iis.u-tokyo.ac.jp (M. Sung).

0360-1323/$ – see front matter © 2010 Elsevier Ltd. All rights reserved.
doi:10.1016/j.buildenv.2010.03.007

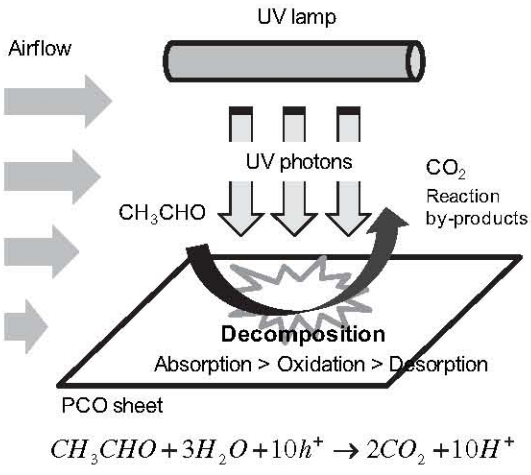

$$CH_3CHO + 3H_2O + 10h^+ \rightarrow 2CO_2 + 10H^+$$

Fig. 1. Acetaldehyde decomposition mechanism of PCO reactor.

with the radiation heat transfer method using view factors and the Monte-Carlo method [14,15]. Hossain has applied a series of numerical methods to designing PCO reactors and Mo also has developed a general numerical model considering convection, diffusion and reaction equations [16,17].

In this study, a PCO reactor featuring newly developed PCO sheets having prismatic crystals of TiO_2 for increasing the reaction area without binder and intended for installation in the duct was considered to improve its efficiency at removing chemical contaminants from indoor air by changing the shape of the reactor unit. The performance of the PCO reactor is dependent on how the target compounds are carried onto the surface of the PCO sheets for photocatalytic oxidation by convection and diffusion, which is closely related to the shape of the reactor. Therefore, the designing of the PCO reactor and detailed considerations to improve the reaction performance of the reactor prior to experimental considerations were performed sequentially using both UVC radiation calculation and CFD simulations. Experiments were also performed to verify the selections by CFD simulation.

2. Methodology

2.1. PCO reactor and UVA intensity

The PCO reactor was initially designed to efficiently utilize the UV irradiation from a UVA lamp. As shown in Fig. 2a, a UVA lamp installed vertically across the airflow direction irradiates UV onto the PCO sheets folded and shaped into triangles in the reactor. As a result, both sides of the PCO sheets can be used for photocatalytic oxidation with one UVA lamp. The width and depth of the PCO reactor are 29 cm and 12.5 cm respectively, and a 10-W UVA lamp (National FL10BL-B), which has a UV output of 1.2 W, was used. The simulations and experiments to estimate the acetaldehyde removal performance targeted only one triangular unit of 7 cm width as all the triangular units have the same shape as shown in Fig. 2b.

The UVA intensity distribution on the surface of the PCO sheets was calculated using RADIANCE, a sophisticated ray-tracing code developed by Lawrence Berkeley National Laboratory [18] and it was used to compare UVA intensity distribution of several initial cases and to checked if there is a black zone where the UVA intensity is low. Only one of the three (RGB) channels in RADIANCE was used for the UVA calculation, and the source output and the properties of the materials for UVA were used in the calculation.

2.2. CFD simulation for the case selection

A triangular unit of the PCO reactor was modeled for the CFD simulation and some alternatives were also introduced to increase the performance of the PCO reactor as shown in Fig. 4 and Table 1. Case A is the basic model with no obstacles in the inlet and outlet openings as shown in Fig. 3b. Case B was designed with obstacles of 0.4-cm width set on the rim of the inlet and outlet openings, so that the air flowing into the unit circulates behind the obstacle, thus increasing contact by the contaminated air on the PCO sheets. By contrast, Case C was designed to set obstacles in the center of the inlet and outlet openings so that more air would come into contact with the PCO sheets at the inlet and outlet. Cases D and E used the same concept, except that the width of the inlet was narrower. In each case, the air velocity at the inlet was set to from 0.1 m/s to 1.0 m/s on the basis of Case A so as to check the effect of the air volume passing through the PCO unit. Acetaldehyde, which is usually considered to be one of the typical indoor air VOCs, was used as the contaminant to be removed.

Airflow was solved using the Reynolds Averaged Navier–Stokes turbulence model, specifically, the standard low Reynolds k–ε model and the governing equation of mass transfer of acetaldehyde, which was treated as a scalar contaminant is as follows.

$$\frac{\partial C_A}{\partial t} + \frac{\partial U_j C_A}{\partial x_j} = \frac{\partial}{\partial x_j}\left(\frac{\nu_t}{Sc}\frac{\partial C_A}{\partial x_j}\right) + R_A \quad (1)$$

where C_A is the mass fraction of acetaldehyde [kg/kg], R_A is the decomposition rate of acetaldehyde [kg/s] on the surface of the PCO sheets, Sc is the turbulence Schmidt number [-], and ν_t is the turbulence viscosity [m^2/s]. The diffusion coefficient for acetaldehyde which could be expressed with the ratio of ν_t to Sc was assumed as 1.16×10^{-5} [m^2/s]. All the acetaldehyde was assumed to be removed completely on the surface of the PCO sheet, as the removal performance of the PCO sheet under various conditions has not yet been confirmed. Commercial software, STAR-CD 4.06, was used for the calculations, and the conditions of the CFD simulation are shown in Table 2.

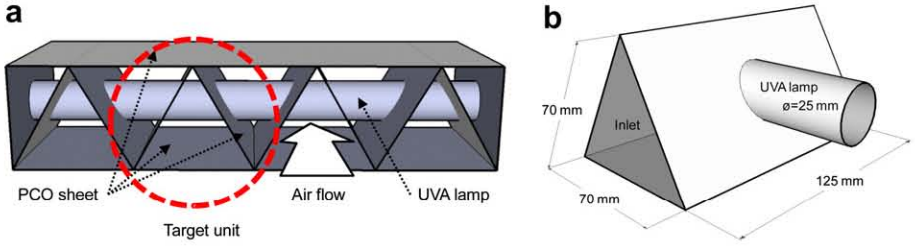

Fig. 2. PCO reactor for air-cleaning: a) entire PCO air-cleaning unit; b) target unit (Case A).

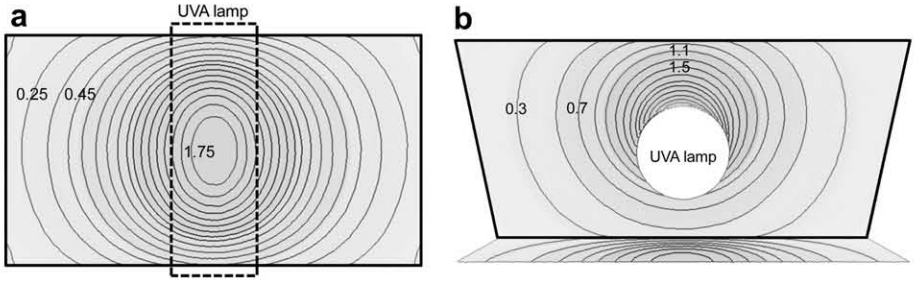

Fig. 3. UVA intensity distribution [mW/cm^2]: a) bottom surface A; b) inclined surface B.

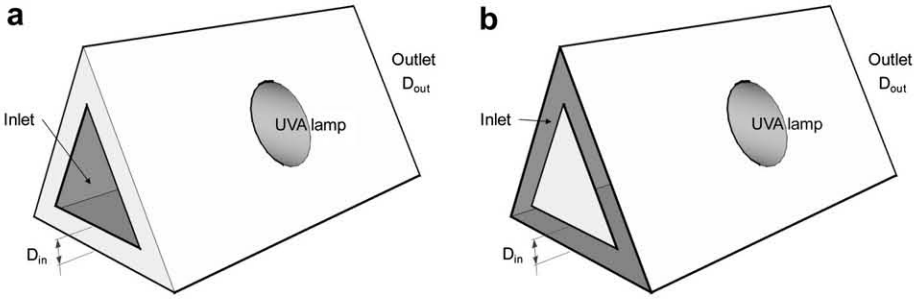

Fig. 4. PCO unit for CFD simulation: a) Case B; b) Cases C–E.

2.3. Experimental setup

Experiments were conducted with the setup shown in Fig. 5 to verify the differences in removal rates among these cases. Gaseous acetaldehyde of a known concentration was mixed with clean air, whose humidity had been controlled in advance, in order to supply air-containing acetaldehyde at a constant concentration, and the contaminated air was supplied to the PCO unit at a controlled flow rate. The temperature and relative humidity of the air flowing through the system were maintained at about 22 °C and 40% respectively. The system was operated for about 10 min without turning on the UVA lamp in the PCO unit in order to stabilize the concentration of air flowing through the system and to check the initial concentration of acetaldehyde when stabilized. Acetaldehyde was detected using a photoacoustic multi-gas monitor (INNOVA 1412) at the outlet line and the initial concentration was set to 1 ppm. The UVA lamp was then turned on to activate the PCO reaction, and the concentration of acetaldehyde was monitored at the outlet line until the concentration stabilized. The concentration was averaged for 10 min after it stabilized and this was used to calculate the removal rate of the PCO unit.

PCO units were prepared for experiments based on the designs introduced for the CFD simulation, in which the basic Case A and Cases D and E, which had shown higher removal rates, were prepared for experiments and tapers and extensions were supplemented to the PCO unit to connect it to the stream line as shown in Fig. 5b. The air velocity was also varied from 0.1 m/s to 1.0 m/s on the basis of Case A during the experiments to verify its effect.

Table 1
CFD simulation cases.

Case	Area of inlet	Area of outlet	D (width of inlet or obstacle)
A	21.2 cm^2	21.2 cm^2	–
B	13.7 cm^2	13.7 cm^2	0.4 cm
C	13.5 cm^2	13.5 cm^2	0.8 cm
D	7.6 cm^2	7.6 cm^2	0.4 cm
E	4.0 cm^2	4.0 cm^2	0.2 cm

3. Results

3.1. UVA intensity

Fig. 3 shows the results of UVA intensity distributions on each PCO sheet surface, and the UVA intensities on the bottom surface (A) ranged from 1.76 to 18.0 W/m^2, while those of the inclined surface (B) ranged from 1.4 to 26.2 W/m^2, and there was no shadow zone.

3.2. CFD simulation

Fig. 6 shows the airflow and the distribution of acetaldehyde concentration in Cases A, B and E. In Case A, the airflow is mainly shown passing under the UVA lamp at low air velocity (Fig. 6a), but as the velocity increases, airflow over the UVA lamp also increases (Fig. 6c). When the air velocity is slow, the overall distribution values of acetaldehyde concentration are low, especially where it can be seen that the concentration around the upper side of the UVA lamp is lower than the lower side (Fig. 6b). In the case where the air velocity is high, the gradient of the concentration near the surface of the PCO sheets is dull, which results in a high concentration overall (Fig. 6d). It can be assumed that the contaminants contained in the air stream have less chance of contacting the surface of the PCO sheets and being oxidized at high velocity compared to at low velocity. In Case B

Table 2
Conditions of CFD simulation.

	Conditions
Mesh	About 340,000 cells (polyhedral)
Turbulence model	Standard low Reynolds k-ε model
Boundary conditions	<Supply> $k_{in}=3/2\times(U_{in}\times 0.05)^2$, $\varepsilon=C_u\times k_{in}^{3/2}/l_{in}$ U_{in}: inlet velocity, C_u = 0.09, l_{in}: length of opening/7 <Exhaust> mass balanced <Wall> no slip, $Y^+<1$
Scalar contaminant	Acetaldehyde (diffusion coefficient: 1.16e-5 m^2/s in 22C air) Inlet concentration: 1 [-]

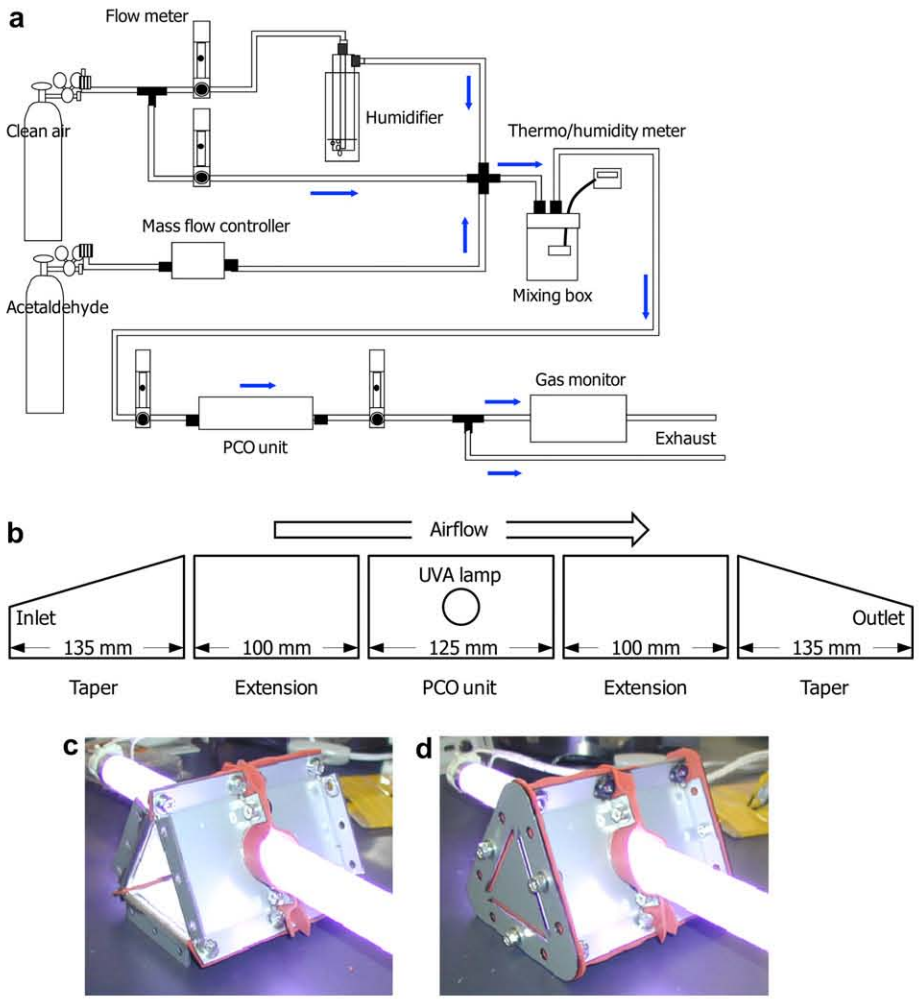

Fig. 5. Experimental setup: a) of entire experimental system; b) PCO unit; c) Case A; d) Case E.

in which obstacles were installed on the rim of the inlet and outlet openings, the air velocities were increased a little near the inlet and outlet openings (Fig. 6e and g), but the concentration on the surface of the PCO sheets, especially near the inlet and outlet openings, has decreased (Fig. 6f and h). In Case E in which obstacles were installed at the inlet and outlet openings, the airflows near the inlet and outlet openings show increased velocity (Fig. 6i and k). The air velocity at the inlet opening is actually much higher than that of Case A as the airflow rates were equalized in both cases. But the widths of the inlet and outlet openings are very narrow, so more contaminants are assumed to be delivered and make contact with the surface of the PCO sheets near the inlet and outlet openings, which results in an overall decrease in concentration compared to Case A (Fig. 6j and l).

Removal rates for each case and velocity were calculated as shown in Table 3. Removal rates (R) were calculated using the following equation.

$$R = \frac{C_{\text{inlet}} - C_{\text{outlet}}}{C_{\text{inlet}}} \times 100 = \left(1 - \frac{C_{\text{outlet}}}{C_{\text{inlet}}}\right) \times 100 \qquad (2)$$

where C_{inlet} and C_{outlet} are the average concentrations of acetaldehyde at the inlet and outlet respectively. In all cases, as the air velocity increases, the removal rate decreases. The removal rates for Case B in which obstacles were installed on the rim of the inlet and outlet openings range from 36.3% to 13.8% and are lower than those of Case A ranging from 41.6% to 15.4%. But Cases C–E show higher removal rates compared to those of Case A, and the narrower the width of the inlet and outlet openings, the higher the removal rates become.

3.3. Experiments

The results of the experiments are shown in Fig. 7. In Case A, the removal rates range from 28% to 7% depending on the inlet velocity. The removal rates for Case D do not show significant differences from those of Case A even at low air velocity, but Case E in which the widths of the inlet and outlet openings are narrower than Case D show higher removal rates ranging from 37% to 4.2% except at a velocity of 1 m/s. Overall, the experimental removal rates were far lower than those calculated in the CFD simulation.

4. Discussion and conclusions

Several alternate designs for a PCO reactor were evaluated using both CFD simulation and experiments to find the design offering the highest removal rate. The installation of obstacles in the middle of the inlet and outlet openings improved the removal performance of the PCO reactor as it increased the air circulation in the reactor and consequently the chance of the acetaldehyde contacting the surface of the PCO sheet. The removal performances were comparatively high in the cases that the obstacles were installed in the center of inlet and outlet openings, which showed that

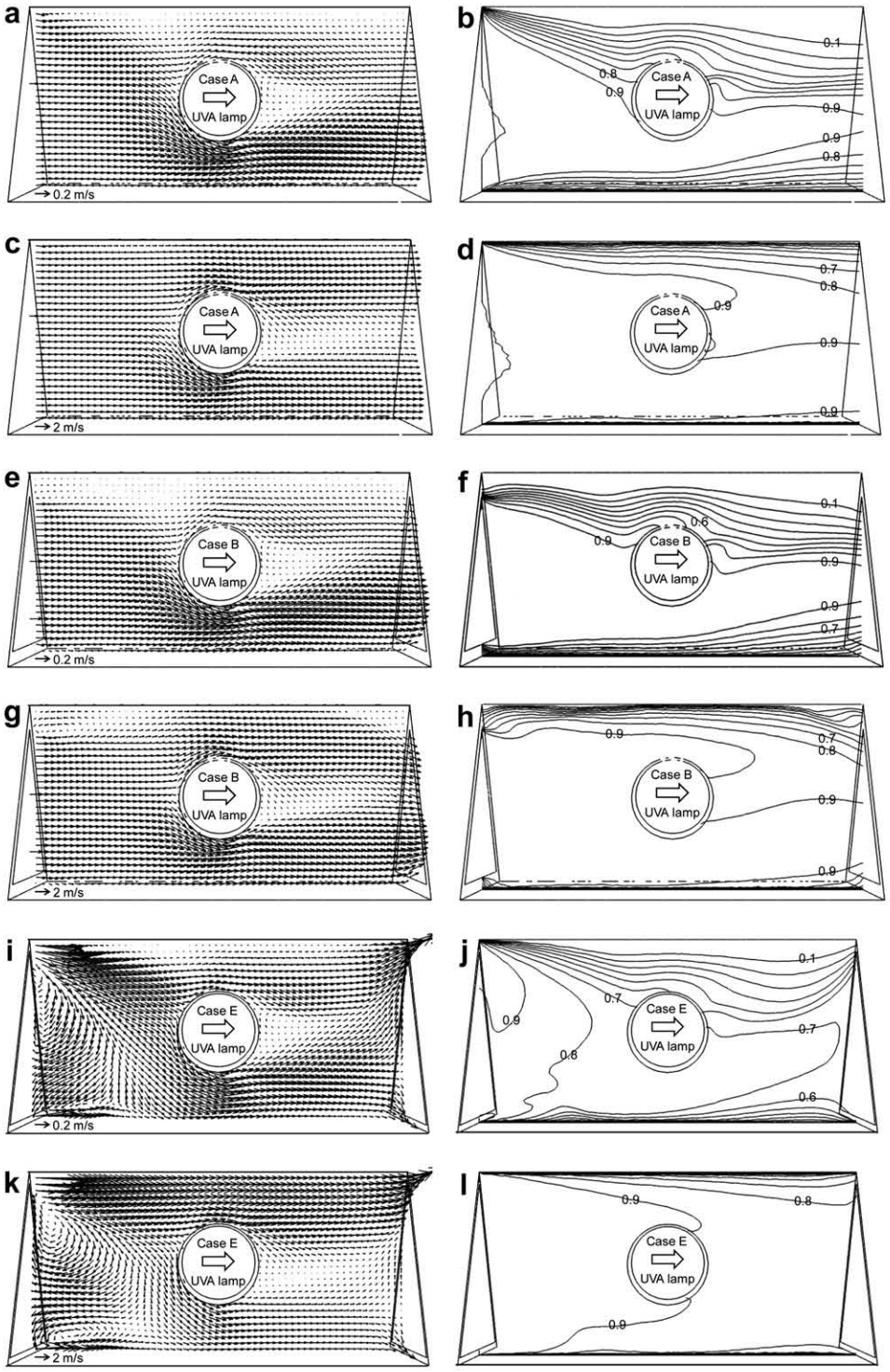

Fig. 6. Distributions of air velocity (a, c, e, g, i, k) and acetaldehyde concentration (b, d, f, h, j, l) calculated using CFD simulation: a, b, d, e, h, i with the same airflow corresponding to Case A with inlet velocity of 0.1 m/s and c, d, f, g, j, k of 1.0 m/s.

convective mass transfer on the PCO sheets near the inlet and outlet played more important role.

However, the experimental performances were not as good overall as had been suggested by the CFD simulation. Whereas the oxidation rate on the surface of the PCO sheet was assumed to be 100% in the CFD simulation, the actual oxidation rates could change according to the UV intensity, concentration of the contaminants, environmental conditions, and characteristics of the photocatalyst, consequently resulting in such differences [19]. The availability of simultaneous oxidation on a PCO surface is limited and when the contaminants delivered reached the limitation, decomposition by the oxidation would stagnate. Moreover, the distribution of UVA intensity on the PCO surfaces can cause discrepancies in local oxidation efficiency.

In many prior research papers, the reaction rates for photocatalysts have been expressed in terms of the Langmuir–Hinshelwood model that could be induced from a wealth of experimental data. The characteristics of PCO sheets, which can be obtained from

Table 3
CFD simulation results for acetaldehyde removal rates by PCO unit.

Case	Inlet velocity* [m/s]				
	0.1	0.2	0.3	0.5	0.1
A	41.6%	34.1%	29.2%	23.0%	15.4%
B	36.3%	29.6%	25.4%	20.1%	13.8%
C	47.0%	38.3%	32.7%	25.5%	17.0%
D	52.5%	43.3%	37.0%	28.9%	19.9%
E	58.7%	48.3%	41.3%	32.9%	24.1%

*Inlet velocities of each case mean the same airflow rate as the inlet velocity for Case A.

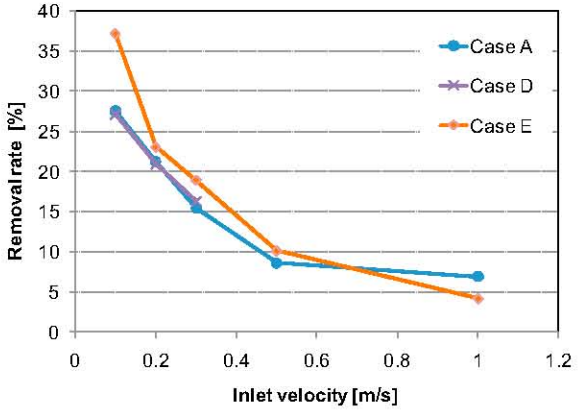

Fig. 7. Experimental results for acetaldehyde removal rates by PCO unit. *Inlet velocities of each case mean the same airflow rate as the inlet velocity for Case A.

experiments as follows, need to be considered for a more accurate CFD simulation. At first, the UV intensity sufficient to oxidize VOCs in contact with PCO sheets needs to be identified, and moreover, as UV intensities on the surface near the inlet and outlet are lower than those right under the UVA lamp, for improved cases such as C–E, the oxidation performance on the surface near the inlet and outlet are quite important. Secondly, the extent to which the initial concentration of VOCs affects the oxidation performance of the PCO sheet should be identified.

Nevertheless, CFD simulation was assumed to be a good method to select the optimal of many alternative PCO reactors.

References

[1] Ministry of Land, Infrastructure and Transport of Japan. Article on the monitoring results of indoor air chemical contaminants, http://www.mlit.go.jp/kisha/kisha06/07/071130_.html; 2006. 2010.3.
[2] International Agency for Research on Cancer. Complete list of agents evaluated and their classification, http://monographs.iarc.fr/ENG/Classification/index.php. 2010.3.
[3] Stedman RL. Chemical composition of tobacco and tobacco smoke. Chemical Reviews 1968;68(2):153–207.
[4] Hodgson AT, Destaillats H, Sullivan DP, Fisk WJ. Performance of ultraviolet photocatalytic oxidation for indoor air cleaning applications. Indoor Air 2007;17:305–16.
[5] Tomida T, Okada N, Katoh M, Katoh S. Adsorption and photocatalytic decomposition of volatile compounds on photocatalyst of TiO_2-silica beads. Adsorption 2005;11:865–9.
[6] Ginestet A, Pugnet D, Rowley J, Bull K, Yeomans H. Development of a new photocatalytic oxidation air filter for aircraft cabin. Indoor Air 2005;15(5):326–34.
[7] Obuchi E, Sakamoto T, Nakano K, Shiraishi F. Photocatalytic decomposition of acetaldehyde over TiO_2/SiO_2 catalyst. Chemical Engineering Science 1999;54(10):1525–30.
[8] Zhao J, Yang X. Photocatalytic oxidation for indoor air purification: a literature review. Building and Environment 2003;38(5):645–54.
[9] Liu Z, Zhang X, Noshimoto S, Murakami T, Fujishima A. Efficient photocatalytic degradation of gaseous acetaldehyde by highly ordered TiO_2 nanotube arrays. Environmental Science and Technology 2008;42:8547–51.
[10] Sakamoto K, Tonegawa Y, Ishitani O. Destruction of indoor air pollutants in TiO_2-wall coated cylindrical flow reactor under 254-nm UV irradiation. Journal of Advanced Oxidation Technologies 1999;4(1):35–9.
[11] Mo J, Zhang Y, Xu Q, Lamson JJ, Zhao R. Photocatalytic purification of volatile organic compounds in indoor air: a literature review. Atmospheric Environment 2009;43(14):2229–46.
[12] Mo J, Zhang Y, Yang R, Xu Q. Influence of fins on formaldehyde removal in annular photocatalytic reactors. Building and Environment 2008;43:238–45.
[13] Obee TN. Photooxidation of sub-parts-per-million toluene and formaldehyde levels on Titania using a glass-plate reactor. Environmental Science and Technology 1996;30:3578–84.
[14] Hossain MM, Raupp GB. Radiation field modeling in a photocatalytic monolith reactor. Chemical Engineering Science 1998;53(22):3771–80.
[15] Singh M, Salvado-Estivill I, Puma GL. Radiation field optimization in photocatalytic monolith reactors for air treatment. American Institute of Chemical Engineers 2007;53(3):678–86.
[16] Hossain MM, Raupp GB, Hay SO, Obee TN. Three-dimensional developing flow model for photocatalytic monolith reactors. American Institute of Chemical Engineers 1999;45(6):1309–21.
[17] Mo J, Yang R. Novel insight into VOC removal performance of photocatalytic oxidation reactors. Indoor Air 2005;15:291–300.
[18] Lawrence Berkeley National Laboratory. The Radiance lighting simulation and rendering system, http://radsite.lbl.gov/radiance/HOME.html. 2010.3.
[19] Yu KP, Lee G, Huang WM, Wu C, Yang S. The correlation between photocatalytic oxidation performance and chemical/physical properties of indoor volatile organic compounds. Atmospheric Environment 2005;40:375–85.